Journal of the European Ceramic Society 16 (1996) 975–984

S0955-2219(96)00009-X
0955-2219/96/$15.00

Slip Casting of Submicron $BaTiO_3$ Produced by Low-Temperature Aqueous Synthesis

Marco Alvazzi Delfrate,[a] Jacques Lemaitre,[a]* Vincenzo Buscaglia,[b] Marcello Leoni[b] & Paolo Nanni[c]

[a] Ecole Polytechnique Fédérale de Lausanne (EPFL), Laboratoire de Technologie des Poudres, MX-Ecublens, CH-1015 Lausanne, Switzerland
[b] Istituto di Chimica Fisica Applicata dei Materiali, CNR, Area della Ricerca, via de Marini 6, I-16149 Genova, Italy
[c] Istituto di Chimica, Facoltà di Ingegneria, Università di Genova, P. le Kennedy, I-16129 Genova, Italy

(Received 24 April 1995; revised version received 15 December 1995; accepted 5 January 1996)

Abstract

Two submicron $BaTiO_3$ powders of different stoichiometries, prepared by an aqueous method have been characterized and submitted to chemical, thermal and mechanical treatments in order to optimize the processing conditions. Acid cleaning at different pH values, calcinations at different temperatures and ultrasonication were performed. The resulting powders were characterized by TGA, SEM, specific surface area, XPS and particle size analysis.

Fired samples were obtained via slip casting and isothermal or non-isothermal sintering. Densification was studied by dilatometric measurements.

Acid cleaning treatments caused desintering phenomena and low fired density, while high density samples with an homogeneous fine grained microstructure were obtained from powders calcined at 950°C.

Deux poudres submicroniques de $BaTiO_3$ de stoechiométries différentes, préparées par synthèse en milieux aqueux, ont été caractérisées et soumises à des traitement chimiques, thermiques et mécaniques pour optimiser la mise en oeuvre. Des lavages acides à différents pH, des calcination et des traitements aux ultrasons ont été effectués. Les poudres résultantes ont été caractérisées par TGA, SEM, mesure de surface spécifique, XPS et granulométrie.

Des corps compacts ont été obtenus par coulage en barbotine et frittage isotherme ou non isotherme. Le comportement au cours du frittage a été étudié par dilatométrie.

Les lavages acides ont provoqué des phénomènes de défrittage et des basses densités, tandis que des échantillons de haute densité présentant une microstructure fine et homogène ont été obtenus à partir de poudres calcinées à 950°C.

1 Introduction

Barium titanate is a ferroelectric material widely employed in the fabrication of multilayer capacitors (MLC), because of its high permittivity. The general trend in ceramic capacitor production is to decrease size and price while preserving or, if possible, increasing performances. This goal can be achieved by a careful control of microstructure and impurity content. Several preparation routes, alternative to the classic solid state reaction $BaCO_3 + TiO_2 \rightarrow BaTiO_3$, have been developed in order to obtain submicron and monodispersed powders, which would produce high density, regular, small grain microstructure free of anomalous grain growth. Among them, the hydrothermal processes[1] are particularly interesting because they allow the production of pure and fine powders and an easy introduction of specific dopants.

The surface of the resulting $BaTiO_3$ powders is contaminated by carbonates, whose presence can be due to the synthesis itself, to the subsequent washing and drying treatments, and to exposure to atmospheric CO_2. This layer, which can promote the formation of agglomerates, has been found to be detrimental to formation and sintering of some commercial powders.[2,3]

Barium titanate powders were prepared by low-temperature (80°C) aqueous synthesis in ICFAM-CNR Genova according to the following reaction:[4]

$$Ba(OH)_2 \cdot H_2O + TiCl_4 + 4NaOH \rightarrow BaTiO_3 + 4NaCl + 4H_2O.$$

NaOH is in 1·5 stoichiometric excess to neutralize HCl and keep the pH high. After 5 h digestion at

* To whom correspondence should be addressed.

constant temperature, the suspension was cooled down and washed several times with distilled water until neutrality was reached. These powders present high specific surface areas, a cubic lattice according to X-ray diffraction (XRD), but lower symmetry and bulk hydroxyl groups according to Raman spectroscopy,[5] and a nearly spherical morphology; the presence of carbonates was detected by XRD. Cristallite size control can be achieved by changing some reaction parameters, such as temperature and digestion time. Sintered samples were prepared by forming such powders by isostatic pressing, obtaining satisfactory ceramic and dielectric properties.[6]

The aim of this work is to optimize the processing conditions and surface treatments of these powders, in order to obtain slip-cast products with good ceramic properties (fine monodispersed grains and high density).

2 Experimental Procedures

Two different batches with different stoichiometries were used: batch BTN5, prepared with stoichiometric quantities of reactants, has a ratio Ti/(Ba+Sr) = 1·05, as measured by plasma spectrometry (ICP) after fusion in $Li_2B_4O_7$; batch BTN8, prepared with an excess of $Ba(OH)_2$, gives Ti/(Ba+Sr) = 0·99; small amounts of Na, probably incorporated during the synthesis, are also detected (≅ 1000 ppm).

Thermal, chemical and mechanical treatments were performed, in order to break agglomerates and obtain high green-density samples.

Partial elimination of water and of carbonates was performed by calcining the powders in a tube furnace for 1 h in air at two different temperatures, either 600 or 950°C (heating rate 10°C/min), using alumina crucibles.

Chemical treatment was performed on non-deagglomerated calcined powder (Batch BTN5) in order to finish the surface decontamination treatment.[2]

Three cleaning solutions were used:

(i) Boiled demineralized water, as a reference;
(ii) pH = 4·5: 0·36 M buffer solution of 50 mol% acetic acid (Merck 100%) + 50 mol% ammonium acetate (Merck 98%) in boiled demineralized water;
(iii) pH = 3·0: 0·30 M buffer solution of 60 mol% nitric acid (Merck 100%) + 40 mol% ammonium citrate (Merck 98%) in boiled demineralized water.

Two grams of powder were cleaned with 55 ml of cleaning solution; these amounts were determined from $BaCO_3$ contents in raw powder, estimated from thermogravimetric (TGA) measurements, and assuming the consumption of 20% of the acid during dissolution.

The suspensions were stirred at 150 rpm and maintained at fixed temperature.

The effects of acid cleaning conditions on the impurity content of the raw powder (namely [C] and [S]) were studied using a 2^4 statistical factorial design. The factors investigated were: (a) pH of the cleaning solution (3–4·5); (b) solution renewal after 2 h of cleaning (no–yes); (c) washing time (8–16 h); and (d) temperature (30–40°C).

After cleaning, the powder suspensions were centrifuged at 4000 rpm for 10 min. The supernatant was discarded and replaced by boiled demineralized water. Washing was repeated until constant conductivity (Schott CG858) of the supernatant was obtained.

Deagglomeration was performed by ultrasonicating 2·5 g of powder suspended in 50 ml of boiled demineralized water for 10 min at constant temperature (Bandelin UW 200 ultrasonic horn).

In order to avoid powder reagglomeration due to capillary forces upon drying, the deagglomerated suspensions were freeze-dried (CHRIST Alpha 1-4), and finally kept in a dessicator under a primary vacuum using $CaCl_2$ as a desiccant (32% relative humidity) until constant weight was reached.

Liquid limits (i.e. the minimum liquid/solid ratio necessary to obtain a free flowing mixture) were determined using 2·00 g of powder mixed with 200 μl of dispersing liquid, vibrating for 1 min at 35 Hz and adding successive 20 μl aliquots of dispersing liquid until the resulting dispersion flows under its own weight.

Slip cast specimens were prepared by mixing 2·00 g of powder with a volume of dispersing solution in excess by 50 μl/g over the measured liquid limit (aqueous solution of PAA with a neutralization ratio R = $[NH_3]/[PAA]$ = 1·5).[7] The slips were vibrated for 1 min at 35 Hz, ultrasonicated (P = 300 W, 7 l bath) for 10 min and outgassed for 1 min under a vacuum. The slips were cast in a silicone rubber mould placed on a flat gypsum base prevented against direct contact with the specimens by inserting a 0·2 μm cellulose membrane. Samples were prepared in this way in the form of blocks (approximately 12·5 × 6·5 × 6·5 mm) for dilatometry measurements, or in the form of discs for microscope observation. The samples were withdrawn from the mould after some hours, and dried to constant weight over $CaCl_2$ in a desiccator.

The processing parameters were studied using a 2^{5-1} statistical factorial design. The factors investigated were: (a) PAA concentration in the slip solution (0·8–1.0%); (b) calcination temperature (600–950°C), (c) cleaning medium (water–acid) — acid cleaning conditions giving the lowest carbon

content according to acid cleaning experience were chosen; (d) powder batch (BTN5-BTN8); and (e) ultrasonic horn power (80–120 W).

Thermogravimetric and differential thermal analyses (TGA-DTA) were performed simultaneously under flowing oxygen atmosphere (SETARAM 92-16.18): 200 mg of powder were weighed in a platinum crucible, and the temperature was raised up to 1000°C at 10°C/min and then up to 1400°C at 5°C/min.

Specific surface areas were measured by N_2 adsorption according to the BET model (Micromeritics type GEMINI 2360). Two grams of powder previously outgassed for 1 h at 200°C in flowing N_2, were used for each measurement.

Granulometry: a 20 mg powder suspension dispersed in a polyacrylic acid aqueous solution ([PAA] = 0·01% and R = 1·5) was used to determine the particle size distributions (HORIBA CAPA-700 cuvet photo centrifuge). Before measurement the suspensions were ultrasonicated for 10 min (P = 150 W, 7 l bath).

Evolved gas analyses (EGA) were carried out on a specific carbon + sulphur analyser (LEYBOLD-HERAEUS type CSA 2003): 0·1 g of powder, mixed with melting agents (1 g Fe + 0·5 g W) to ensure complete decomposition, were placed in a crucible in an induction furnace with flowing oxygen. After H_2O separation, the evolved gases were analysed by infra-red detectors specially calibrated for CO_2 and SO_2.

X-ray photoelectron spectroscopy measurements (XPS), (PERKIN ELMER Phi 5500 ESCA system, MgKα line 15 KeV-350 W) were carried out using several milligrams of powder placed on an indium substrate; the signal curves were fitted using Gaussian peaks summation and Shirley baseline subtraction.

Isothermal sintering (Lynn HT 1800G furnace) was carried out for 2 h at different temperatures, corresponding to densification and de-densification peaks, and different heating rates (1 and 10°C/min) were used to reach the sintering temperature.

Green and fired densities were measured by Archimedes' method, using isopropanol as an immersion liquid, and assuming the theoretical density of $BaTiO_3$ to be 6·02 g.cm^{-3}. For green density measurements, the samples were first saturated in a vacuum with isopropanol.

Dilatometric curves were measured under dry air (SETARAM DHT) using the following heating cycle: 10°C/min up to 800°C, 3·3°C/min up to 1400°C and 5°C/min down to room temperature. Intermediate densities were calculated from dilatometric curves corrected for thermal expansion and calibrated on measured final densities.

X-ray diffraction (XRD) (SIEMENS Kristalloflex 805 diffractometer, Ni-filtered Cu–Kα wavelength) was performed with a scanning step of 0.04 2θ and a 4 s sampling time for each point with digital collection of the resulting pattern.

Scanning electron microscopic observations (SEM) were performed by conventional methods (JEOL 6300 and CAMBRIDGE S-360), for both powder and sintered specimen observations. Sintered samples were polished and either thermally (heating up to 1200°C at 20°C/min) or chemically etched (10 min in a 1:1:2 mixture of HCl 37%, H_2O_2 and water).

Statistical analysis: the results of the statistical factorial experiments were analysed by the ANOVA method. The statistical significance of the observed effects is reported as the probability p of a Type I error (i.e. the risk to consider, by mistake, an effect as significant).

3 Results

3.1 X-ray diffraction

XRD spectra of raw powders show a cubic structure as reported in the literature for hydrothermal powders:[8] the diffraction profiles of powders calcined at 950°C tend to shift towards the tetragonal form, but the transition is completed for sintered samples. This effect can be attributed to the presence of internal OH giving sufficient elasticity to the structure to appear cubic to XRD analysis[5,8] and/or to the grain size.[9] $BaCO_3$ peaks are visible for both raw powders and disappear after 950°C treatment.

Second phase peaks are eliminated by both the acid cleaning treatments (pH = 3 and pH = 4·5) and by calcination at 950°C, while calcination at 600°C is ineffective.

3.2 Thermogravimetric analysis

Both raw powders exhibit very similar TGA behaviour (Fig. 1). Chemical and thermal treatments considerably modify the weight loss derivative (Fig. 2). The first DTG peak (150°C) is due to reversibly adsorbed water or CO_2. The second peak (250–300°C), which is partially reduced by acid cleaning, decreases significantly upon calcination at 600°C and is completely eliminated after calcination at 950°C. This behaviour can be related to the elimination of OH groups present in the crystal lattice, as observed by IR spectroscopy.[5] The peak at 950°C disappears after acid cleaning or after calcination at 950°C, while it is left unchanged by calcination at 600°C; therefore, it can be ascribed to the decomposition of $BaCO_3$ also observed by XRD.[2]

3.3 Differential thermal analysis

The DTA signal is noticeably affected by thermal and chemical treatments; Fig. 3 clearly shows the

presence of a liquid phase at about 1300°C for the acid cleaned powders.

3.4 Specific surface area

Specific surface measurements of raw and thermal treated powders are reported in Table 1: no substantial differences are observed between the two batches, both presenting high specific surfaces. After calcination at 950°C the specific surface area is reduced by 70%, of the original value, while calcination at 600°C causes only a 5–10% decrease.

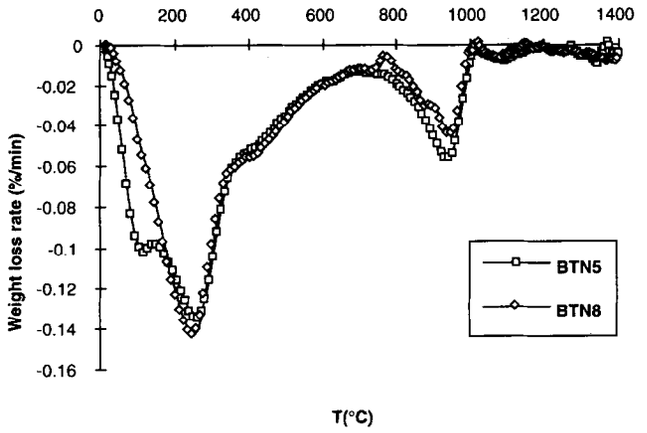

Fig. 1. Weight loss rate curves of raw powders.

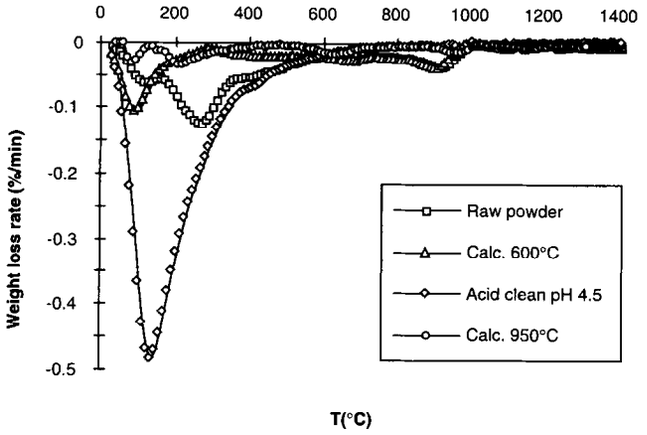

Fig. 2. Weight loss rate curves of powders from BTN5 batch, after various treatments.

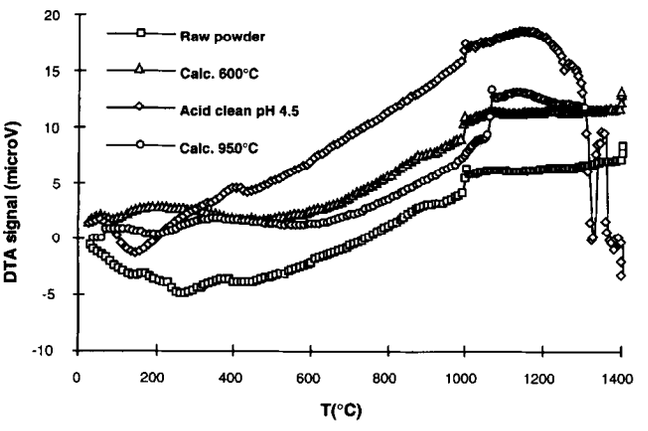

Fig. 3. DTA curves of powders from BTN5 batch, after various treatments.

3.5 Carbon and sulfur contents

EGA measurements have been carried out on raw or thermally treated powders, and powders treated chemically under different conditions: the results are reported in Table 2.

Calcination at 950°C considerably reduces the carbon content while calcination at 600°C gives only a very slight reduction. The sulfur content is low for all the samples (<13 ppm), none of the investigated factors having a significant effect ($p > 0.05$).

As shown in Fig. 4, the most important factor affecting the amount of residual carbon is the washing pH (factor D). Upon washing at pH = 3, precipitation of a sparingly barium citrate salt presumably occurs, thereby increasing the carbon content of the samples; the effect is stronger at a higher washing temperature (factor C); increasing the number of wash runs decreases the carbon content ($p < 0.01$).

The residual carbon content is much lower at pH = 4·5; the results were analysed separately, and are presented in Fig. 5. Here, the residual carbon increases with the wash time (factor B), and with temperature (factor C) ($p < 0.05$); the wash number (factor A) has no significant effect ($p > 0.10$). Thus, in order to minimize the residual carbon content, a single wash at 30°C for 8 h has been applied in the subsequent work.

3.6 XPS analysis

Surface Ba, Ti, O, C and Na contents were determined by XPS analysis on raw and treated powders;[11] the results are summarized in Table 3.

The Na content, calculated from the Na_{1s} transition decreases from about 3% for raw and calcined powders down to 1·1% for powders cleaned with the citric buffer and 0·6% for powders cleaned with the acetic buffer. The carbon content, calculated from the C_{1s} transition, increases from about 14·5% for the raw powders, up to 25% for the powders calcined at 950°C, and 38% for the powders cleaned with the citric buffer.

The Ba/(Ba + Ti) ratio was calculated from the $Ba_{3d5/2}$ and Ti_{2p} transitions. It decreases from about 40% for the raw powders and the powders calcined

Table 1. Specific surface area for raw, 600 and 950°C calcined powders

	Batch	
Treatment	*BTN5*	*BTN8*
Raw	27·2	27·5
Calcined, 600°C	25·9	24·7
Calcined, 950°C	8·5	8·0

Table 2. Residual carbon and sulfur concentrations after different treatments

Test number	*Treatment*	*Wash number*	*Wash time (h)*	*Temperature (°C)*	*pH*	*[C] (wt%)*	*[S] (ppm)*
1	'1'	1	8	30	3·0	6·55	12
2	a	2	8	30	3·0	4·68	7
3	b	1	16	30	3·0	8·61	5
4	ab	2	16	30	3·0	4·91	9
5	c	1	8	40	3·0	10·71	3
6	ac	2	8	40	3·0	6·70	3
7	bc	1	16	40	3·0	10·80	11
8	abc	2	16	40	3·0	8·31	3
9	d	1	8	30	4·5	0·20	2
10	ad	2	8	30	4·5	0·20	1
11	bd	1	16	30	4·5	0·23	4
12	abd	2	16	30	4·5	0·23	2
13	cd	1	8	40	4·5	0·27	1
14	acd	2	8	40	4·5	0·29	1
15	bcd	1	16	40	4·5	0·29	13
16	abcd	2	16	40	4·5	0·28	8
	Raw powder	—	—	—	—	0·27	1
	Calcined, 600°C	—	—	—	—	0·24	3
	Calcined, 900°C	—	—	—	—	0·04	3

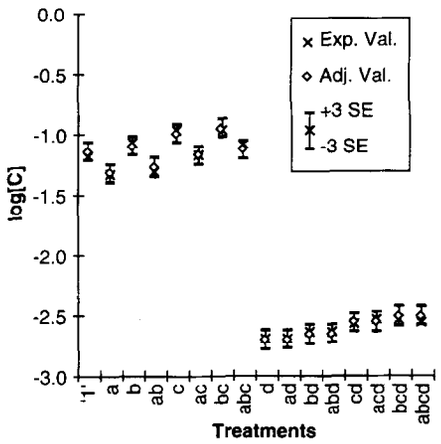

Fig. 4. Carbon content after acid washing (p <0·01).

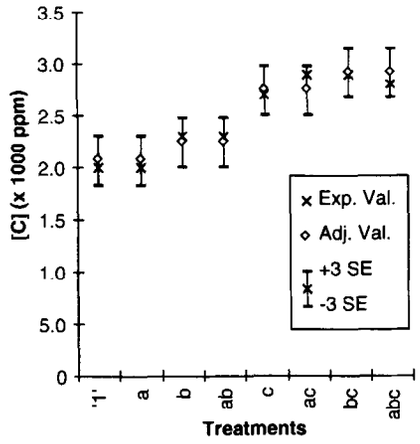

Fig. 5. Carbon content after acid washing at pH = 4·5 (acetic buffer, p <0·05).

at 600°C, down to 33% for the powders cleaned with the acetic buffer, indicating that this treatment has dissolved Ba in the form of Ba^{2+} ions. On the other hand this ratio increases up to about 50% for the powders calcined at 950°C and for those cleaned with the citric buffer. The shapes of the O and C peaks were not investigated in detail, because of their high sensitivity to atmospheric contamination.

The $Ba_{3d5/2}$ peak was resolved as the superimposition of two Gaussian components separated by 1·5 ± 0·1 eV, corresponding respectively to the titanate (the higher energy peak) and the carbonate matrix (the lower energy peak): the ratio $BaCO_3/BaTiO_3$ was calculated from these peaks.[2] Washing in the citric buffer increases the relative height of the carbonate peak, and consequently the thickness of the carbonate layer, by a factor of 10, while 950°C calcination leads to a 50% increase, and acetic buffer cleaning leads to a 40% decrease.

Table 3. XPS analysis (at%) of raw, calcined and acid cleaned powders

Treatment	*C (at%)*	*O (at%)*	*Ba (at%)*	*Ti (at%)*	*Na (at%)*	*Ba / (Ba + Ti)*	*$BaCO_3$ / $BaTiO_3$*
Raw	14·5	58·5	9·8	14·1	3·1	0·41	0·45
Calcined, 600°C	15·3	55·1	10·5	15·8	3·3	0·40	0·50
Calcined, 950°C	24·9	50·4	11·2	9·9	3·6	0·53	0·77
Cleaned, pH3	37·6	47·8	6·8	6·8	1·1	0·50	5·13
Cleaned, pH 4·5	13·5	59·0	9·0	18·0	0·6	0·34	0·30

3.7 Powder morphology

SEM observations showed irregular agglomerates of particles smaller than 100 nm, for both raw and 600°C calcined powders (Fig. 6). Conversely, calcination at 950°C results in compact and large agglomerates, up to 20 μm in size. Sintering has already started and the elementary particles are necked to each other, thereby reducing the specific surface (Fig. 7).

3.8 Green densities

Calcination at 950°C also reduces the liquid limit, while increasing significantly the green density up to 60% of the theoretical density (p <0·01), even though this green density is still lower than the one expected for randomly packed monosized spheres.[12]

On the other hand, the effects of stoichiometry, cleaning solutions (water or acetic buffer), PAA concentration in the dispersing solution, and ultrasonic horn power on these properties were found to be unsignificant (p >0·05).

3.9 Particle size distribution

The particle size distribution of the powder calcined at 950°C, treated with the ultrasonic horn and freeze dried, was measured with correction for light scattering;[13] this was the powder giving the highest green densities (Fig. 8). The median in volume distribution is 0·14 μm, but some agglomerates which can cause low green densities are still present.

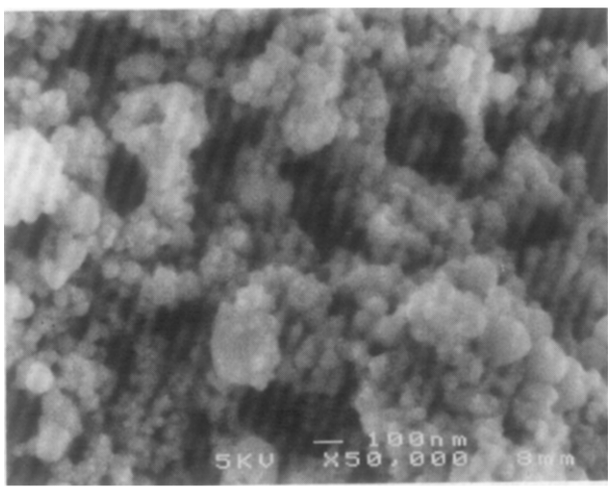

Fig. 6. SEM micrograph of raw powder from BTN5 batch.

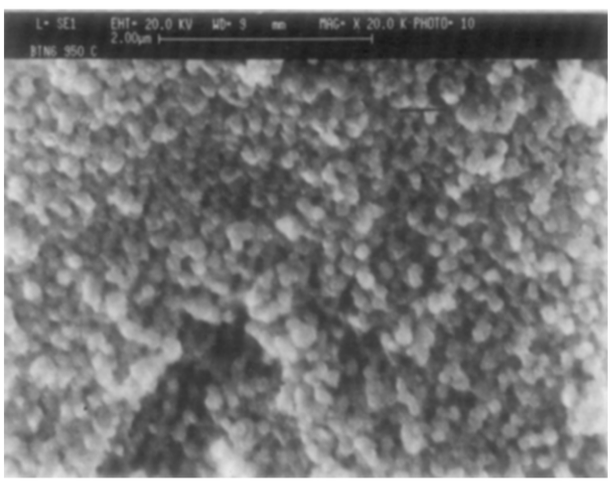

Fig. 7. SEM micrograph of powder from BTN5 batch calcined at 950°C.

3.10 Dilatometry

Dilatometric curves for BTN5 batch are reported in Figs 9 and 10, and in Figs 11 and 12 for BTN8 batch; the main features of these curves are summarized in Table 4. The two batches have the same sintering behaviour, except for the sintering and de-sintering (when present) peak temperatures. De-sintering is always observed with acid cleaned powders, and never with powders washed with demineralized water. For this reason, lower final densities are obtained with acid cleaned powders. The de-sintering phenomenon is less pronounced for the powders calcined at 600°C, probably due to a higher fraction of open porosity at the de-sintering temperature.

Samples from powders calcined at 950°C present starting and maximum densities higher than those calcinated at 600°C: the final density of water cleaned samples ranges between 91–93% and 95–96%, and between 67–74% and 82–86% for acid cleaned samples. Calcination at 950°C decreases by a factor of 2 times the height of the lower temperature sintering peak, because part of the shrinkage has already taken place during the calcination treatment.

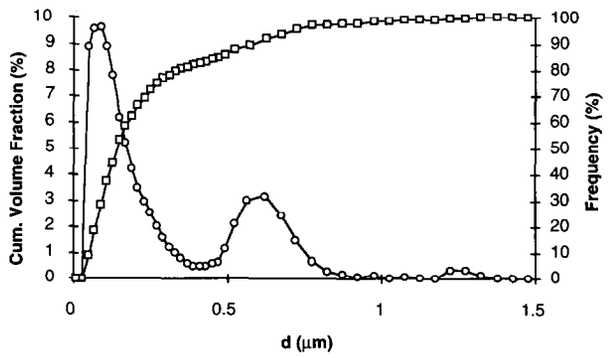

Fig. 8. Particle size distribution of powder from BTN5 batch calcined at 950°C.

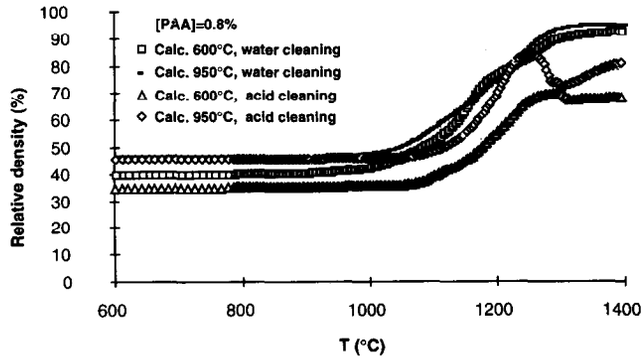

Fig. 9. Densification curves of calcined powders from BTN5 batch.

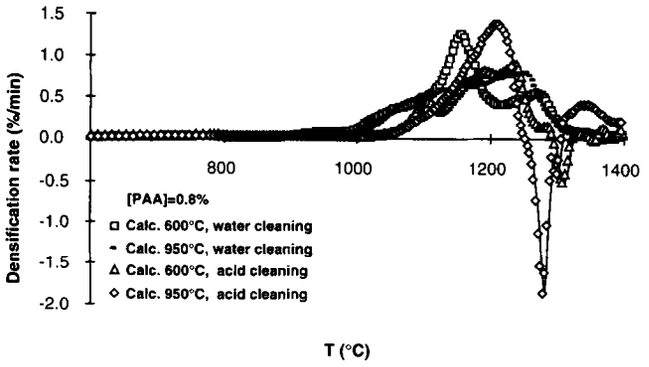

Fig. 10. Densification rate curves of samples from BTN5 batch.

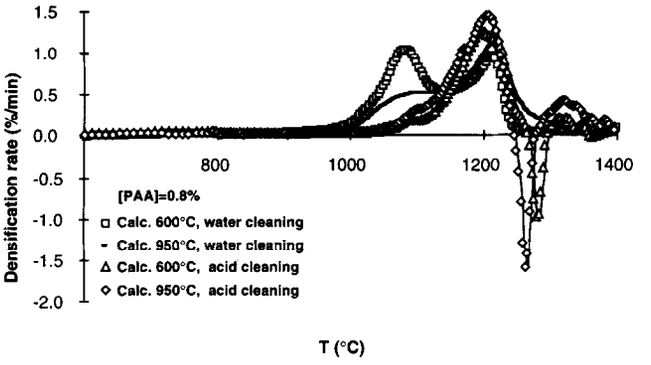

Fig. 12. Densification rate curves of samples from BTN8 batch.

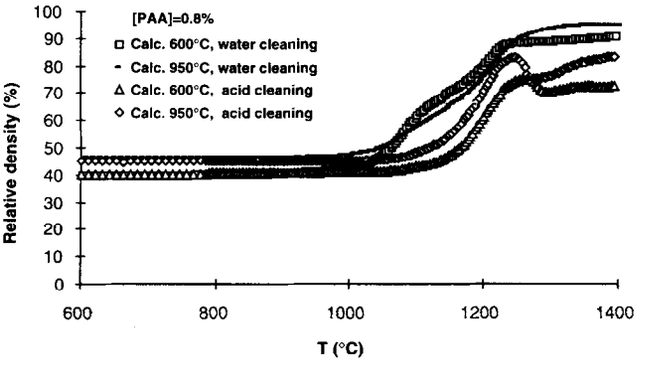

Fig. 11. Densification curves of samples from BTN8 batch.

3.11 Microstructure of sintered samples

SEM observations on non-isothermally sintered samples reveal a coarse-grained structure for water cleaned samples (Fig. 13), whereas acid cleaned samples present coarser grains and pores, probably caused by desintering (Fig. 14). Water cleaned samples sintered 2 h at the first densification peak temperature (Fig. 15) have a very fine grain size (<1 μm), although densification is not complete (≅ 93% theoretical density). The samples sintered at the second densification peak temperature exhibit higher densities: 95 and 97%, depending on the heating rate (10 and 1°C/min, respectively). SEM inspection of these samples reveals a homogeneous and fine-grained microstructure (Fig. 16), although some formation defects are still present (Fig. 17), which decrease density and cause local grain growth. The grain size distribution was measured for these samples: both present a log-normal monomodal distribution. The mean apparent grain diameter, calculated from the measurement of the areas of 350 grains (assuming spherical shape), was 1·4 ± 0·7 μm for the denser sample and 1·2 ± 0·6 μm for the second one.

4 Discussion

No effect on powder and compact properties was detected when the Ti/(Ba + Sr) ratio goes from 1·05 to 0·99, except for a shift in the sintering peak temperatures, which are higher for the Ti-rich batch. Impurities can probably account for this anomalous effect, as the stoichiometry would rather explain the opposite behaviour. Sintering of the raw powders starts at lower temperatures (about 900°C), and induces initially a reorganization of the crystallites together with a reduction of the surface area.

Calcination at 600°C does not lead to substantial changes in the raw powders. It eliminates the irreversible TG loss at 250–300°C and reduces the powder specific surface by about 5–10%. The decrease in surface area is accompanied by an increased surface carbon content, as revealed by XPS measurements: this effect is due to a redistribution of the carbon present on a smaller area, resulting in a

Table 4. Main characteristics of non-isothermal sintering for samples obtained from calcined powders after acid or water cleaning

	Pretreatment conditions		*Sintering characteristics*		
Batch	*Calcinated temperature (°C)*	*Cleaning*	*Maximum density ($\%D_{th}$)*	*Sintered peak (°C)*	*De-sintered peak (°C)*
BTN5	600	Water	93	1157	—
BTN5	950	Water	95	1247	—
BTN5	600	pH 4·5	69	1238	1311
BTN5	950	pH 4·5	83	1210	1280
BTN8	600	Water	91	1082	—
BTN8	950	Water	96	1215	—
BTN8	600	pH 4·5	74	1201	1281
BTN8	950	pH 4·5	82	1208	1264

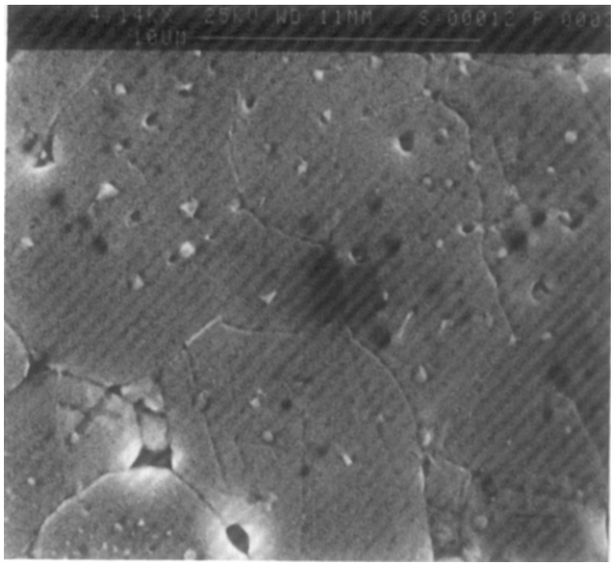

Fig. 13. SEM micrograph of sample non-isothermally sintered (1400°C); BTN8 powder calcined at 950°C and water cleaned.

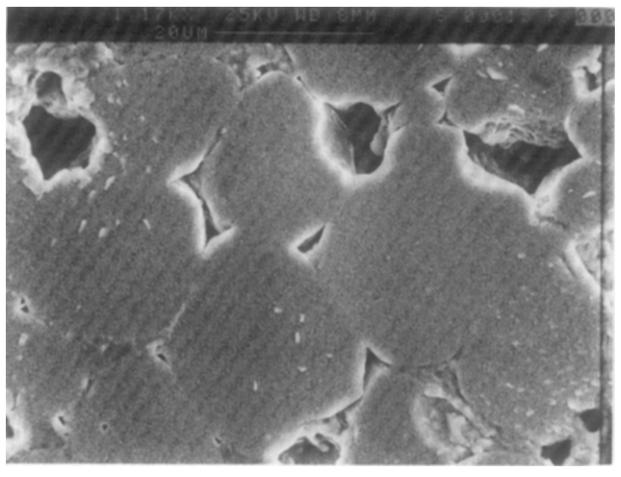

Fig. 14. SEM micrograph of a non-isothermally sintered sample (1400°C); BTN8 powder calcined at 950°C and cleaned with acetic buffer.

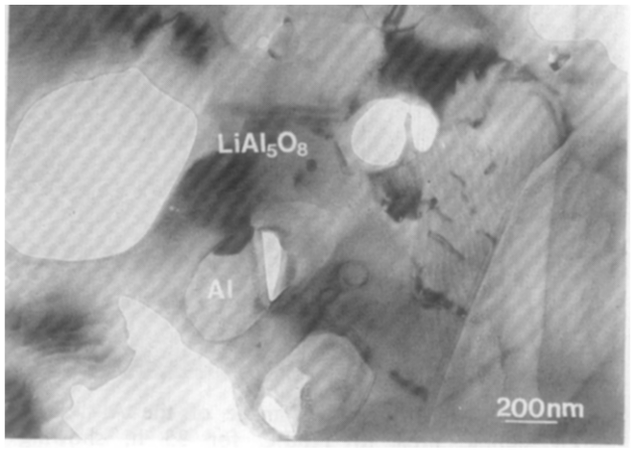

Fig. 15. SEM micrograph of an isothermally sintered sample (2 h, 1167°C, slow heating rate: 1°C/min); BTN5 powder calcined at 950°C and water cleaned (93% theoretical density).

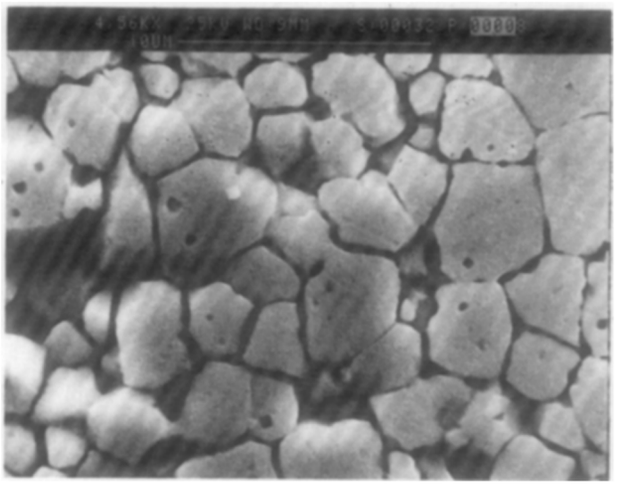

Fig. 16. SEM micrograph of an isothermally sintered sample (2 h, 1247°C, slow heating rate: 1°C/min); BTN5 powder calcined at 950°C and water cleaned (97% theoretical density).

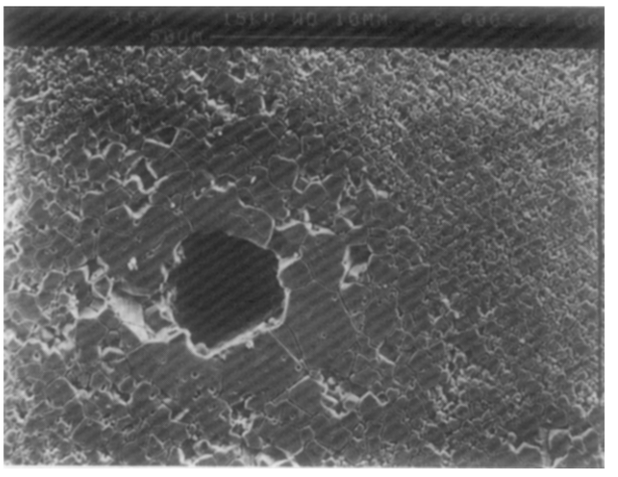

Fig. 17. SEM micrograph showing a forming defect in an isothermally sintered sample (2 h, 1247°C, slow heating rate: 1°C/min); BTN5 powder calcined at 950°C and water cleaned (97% theoretical density).

thicker carbonate layer. EGA measurements provide evidence for a reduction of about 10% in total carbon content. As a consequence, $BaCO_3$ is still present after this thermal treatment.

Calcination at 950°C reduces the surface area by about 70%, thereby increasing the carbon content detected by XPS. However the total carbon content measured by EGA is decreased dramatically from 0·27% down to 0·04%, and TG losses are markedly reduced. $BaCO_3$ is therefore almost completely decomposed, as confirmed by XRD, and the carbon is reduced to a reversibly bounded surface layer. Sintering is already active at this temperature, so that a strong agglomerate can form by inter-crystallite necking, as shown by SEM.

Green bodies made of powders calcined at 950°C have higher densities than those made of powders calcined at 600°C; in any case, however,

the green densities obtained are still low, due to formation defects. The better quality of the green bodies prepared from powders calcined at 950°C leads to higher sintered densities, even though the shrinkage starts at higher temperature. Formation defects and residual agglomerates in water-washed samples are responsible for lower than expected sintered densities, as they lead to the formation of pores with a higher-than-critical coordination number. SEM observation reveals the presence of pores in samples made from powders calcined at 600 or 950°C, though in smaller number for the latter temperature. Despite this residual porosity, densities up to 97% have been achieved at the peak temperature of densification (≅ 1250°C), after 2 h sintering (heating rate 1°C/min). This sintering temperature was quite low, due to the high surface area of the powders, which provides the driving force for shrinkage. The microstructure of these samples is quite interesting, because no evidence for abnormal grain growth is visible and the grain size is quite small (<2 μm).

Acid cleaning at pH = 3, precipitating barium citrate, caused an increase in carbon content instead of the decrease expected: for this reason the citric buffer cannot be recommended as a cleaning medium. The acid cleaning at pH = 4·5 was successful in eliminating partly the surface C and Na, but also dissolved some Ba from the surface. As a result, a Ti-rich surface is formed leading to the development of a liquid phase at about 1300°C, as detected by DTA. In fact, the BaO–TiO_2 system presents a eutectic composition melting at 1317°C,[10] whose melting temperature can be lowered by the presence of impurities.

No effect of chemical treatment was detected on green densities: acid cleaning does not seem to enhance de-agglomeration when the powders are treated with a US horn.

The surface modifications caused by acid cleaning, namely the elimination of a Ba-rich surface layer, lead to a sintering behaviour dramatically different from that of water cleaned powders. The shrinkage start is delayed and a de-sintering step appears, leading to markedly lower final densities. The delay of the onset of densification (from 900 to 1000°C) has been observed previously,[3] and can be ascribed to a more complete consolidation without shrinkage taking place when impurities are removed from the powder surface. The presence of a de-sintering step, absent in water cleaned powders, can be ascribed to the formation of a large amount of liquid phase. The liquid formed enhances the plasticity of the material, allowing a de-sintering process that can be due to CO_2 release[14] and to inhomogeneous densification:[15] lower densities are therefore obtained for acid cleaned powders.

5 Conclusion

The aim of the present work was to investigate the influence of surface treatments in order to obtain dense and small grained sintered samples. Acid cleaning with acetic buffer, which proved a useful method to increase the density of samples prepared from low specific surface area powders (<2 m^2/g),[3] degrades the ceramic properties of high specific surface powders synthesized by low-temperature aqueous precipitation. In fact, green densities are not enhanced compared to powders merely treated by ultrasonication and, in addition, de-sintering considerably reduces the final density. The removal of Ba from the surface should therefore be avoided.

Powders calcined at 950°C, water cleaned and ultrasonicated, can be sintered up to 97% of the theoretical density at relatively low temperatures (≅ 1250°C), with a fine grained homogeneous microstructure. The microstructure obtained is particularly favourable for dielectric properties, especially by comparison to results of similar treatments on commercial powders:[3] research on this promising synthesis route should therefore be continued. Higher fired densities can be obtained by enhancing green density, through elimination of forming defects and agglomerates that are still present. In order to avoid forming defects, the rheological properties of the casting slip should be optimized. Elimination of the agglomerates requires a stronger de-agglomeration technique such as ball-milling, but pollution effects from grinding media must be considered. In addition, the synthesis method, allowing the control of the crystallite size by changing some processing parameters, can also help to enhance the green density.

Acknowledgements

The authors would like to thank Dr C. Hérard and Dr P. Bowen for useful discussions, Mr B. Senior for SEM powder observations, Mr N. Xanthopulos for XPS measurements and Mr F. Rossetti for EGA analysis.

The financial support of the Swiss National Fund for Scientific Research (project no 21-29'914·90) is gratefully acknowledged by J. L.

COTRAO (Communauté de Travail des Alpes Occidentales) is acknowledged for a grant by M.A.D.

References

1. Dawson, W. J., Hydrothermal synthesis of advanced ceramics powders. *Am. Ceram. Soc. Bull.*, **67** (1988) 1673–8.
2. Hérard, C., Faivre, A. & Lemaitre, J., Surface decontamination treatments of undoped $BaTiO_3$. Part I: powder and green properties. *J. Europ. Ceram. Soc.*, **15** (1995) 135–43.

3. Hérard, C., Faivre, A. & Lemaitre, J., Surface decontamination treatments of undoped $BaTiO_3$. Part II: influence on sintering. *J. Europ. Ceram. Soc.*, **15** (1995) 145–53.
4. Nanni, P., Leoni, M., Buscaglia, V. & Aliprandi, G., Low temperature aqueous preparation of barium metatitanate powders. *J. Europ. Ceram. Soc.*, **14** (1994) 85–90.
5. Busca, G., Buscaglia, V., Leoni, M. & Nanni, P., Solid state and surface spectroscopic characterization of $BaTiO_3$ fine powders. *Chemistry of Materials*, **6** (1994) 955–61.
6. Alvazzi Delfrate, M., Leoni, M., Nanni, L., Melioli, E., Watts, B. E. & Leccabue, F., Electrical charaterization of $BaTiO_3$ made by hydrothermal methods. *J. Mater. Sc. Mater. in Electronics*, **5** (1994) 153–6.
7. Chen, Z.-C., Ring, T. A. & Lemaitre, J., Stabilization and processing of aqueous $BaTiO_3$ suspension with polyacrylic acid. *J. Amer. Cer. Soc.*, **75** (1992) 3201–8.
8. Hennings, D. & Schreinemacher, S., Characterization of hydrothermal barium titanate. *J. Europ. Ceram. Soc.*, **9** (1992) 41–6.
9. Uchino, K., Sadanaga, E. & Hirose, T., Dependence of the crystal structure on particle size in barium titanate. *J. Amer. Cer. Soc.*, **72** (1989) 1555–8.
10. Jaffe, B., Cook, W. R. & Jaffe, H., *Piezoelectrics Ceramics*, Academic Press, London and New York, 1971.
11. Hung, C. C., Riman, R. E. & Caracciolo, R., An XPS investigation of hydrothermal and commercial barium titanate powders. In *Ceramic Powder Science III*, **12** (1990) 17–25.
12. Nolan, G. T. & Kavanagh, P. E., Computer simulation of random packings of spheres with log–normal distributions. *Powder Technology*, **76** (1993) 309–16.
13. Bowen, P., Dirksen, J. A., Humphrey-Baker, R. & Jelinek, L., An approach to improve the accuracy of submicron particle size distribution using the Horiba CAPA-700. *Powder Technology*, **74** (1993) 67–71.
14. Demartin, M., Hérard, C., Lemaitre, J. & Carry, C., Grain growth and swelling of hot pressed $BaTiO_3$ during annealing treatments. In *Proceedings of Third Euro-Ceramics*, eds Duran P. & Fernandez J. F., Faenza editrice iberica, Madrid 1993, pp. 775–80.
15. Sudre, O. & Lange, F. F., The effect of inclusions on densification: III the desintering phenomenon., *J. Amer. Cer. Soc.*, **75** (1992) 3241–51.